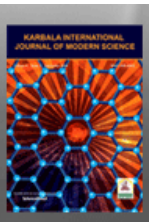
Karbala International Journal of Modern Science

Manuscript 3388

Optimization of The Starch Chitosan-based Flocculant Crosslinked by Ethylene Glycol Dimethacrylate on Removing Dypro 19 Textile Dye from Wastewater

Asep Nurohmat Majalis

Putri Ramadhani

Hendris Hendarsyah Kurniawan

Axel Dimaz Sanusi Pasaribu

Hafiizh Prasetia

See next page for additional authors

Optimization of The Starch Chitosan-based Flocculant Crosslinked by Ethylene Glycol Dimethacrylate on Removing Dypro 19 Textile Dye from Wastewater

Abstract

Dyes used in industry, especially textile dyes, are one of the water pollutants that receive much attention because they are potentially toxic, carcinogenic, mutagenic, and generally challenging to decompose naturally. Textile dyes from wastewater can be removed through coagulation-flocculation. However, conventional coagulation-flocculation based on Fe and Al salts and synthetic polymers often leaves residual pollution. In this research, the performance of the new biopolymer-based flocculant, namely starch-ethylene glycol dimetacrylate-chitosan (SEC), which can act as coagulants and flocculants in solid-liquid separation of textile dyes, has been optimized using response surface methodology (RSM) approach. The influences of several independent variables, such as initial pH, SEC dosage, and rapid stirring time, were studied. The design experiment was the box-Behnken design (BBD), which involved three factors, three levels, and 15 treatment combinations. Based on the fitting results, the quadratic model is significant and accurate in predicting the solid-liquid separation of Dypro 19 (*p*-value 0.0002, F-value 51.94, and R^2 0.9894). Numerical optimization based on the desirability function shows that using initial pH variables of 8, SEC dosage of 2.2 mL L^{-1}, and rapid stirring time of 3 minutes can produce a predicted removal of Dypro 19 of 97.01%. Model validation through experiments on these variables shows that 95.71% of Dypro 19 can be removed. These results indicate that the proposed model's validity, accuracy, and acceptability are good.

Keywords

Optimization; Flocculant performance; Flocculation; Starch-ethylene glycol dimethacrylate-chitosan; Response sur-face methodology; Box-Behnken design; Solid-liquid separation; Textile dye

Authors

Asep Nurohmat Majalis, Putri Ramadhani, Hendris Hendarsyah Kurniawan, Axel Dimaz Sanusi Pasaribu, Hafiizh Prasetia, Fitri Yuliani, Andreas Andreas, and Hartati Hartati

RESEARCH PAPER

Optimization of the Starch Chitosan-based Flocculant Crosslinked by Ethylene Glycol Dimethacrylate on Removing Dypro 19 Textile Dye From Wastewater

Asep N. Majalis [a,*], Putri Ramadhani [a], Hendris H. Kurniawan [a], Axel D.S. Pasaribu [b], Hafiizh Prasetia [a], Fitri Yuliani [a], Andreas Andreas [a], Hartati Hartati [c]

[a] Research Center for Chemistry, National Research and Innovation Agency (BRIN), KST BJ Habibie, South Tangerang, Indonesia
[b] Undergraduate Program of Chemistry, Airlangga University, Surabaya, Indonesia
[c] Department of Chemistry, Airlangga University, Surabaya, Indonesia

Abstract

Dyes used in industry, especially textile dyes, are one of the water pollutants that receive much attention because they are potentially toxic, carcinogenic, mutagenic, and generally challenging to decompose naturally. Textile dyes from wastewater can be removed through coagulation-flocculation. However, conventional coagulation-flocculation based on Fe and Al salts and synthetic polymers often leaves residual pollution. In this research, the performance of the new biopolymer-based flocculant, namely starch-ethylene glycol dimetacrylate-chitosan (SEC), which can act as coagulants and flocculants in solid-liquid separation of textile dyes, has been optimized using response surface methodology (RSM) approach. The influences of several independent variables, such as initial pH, SEC dosage, and rapid stirring time, were studied. The design experiment was the box-Behnken design (BBD), which involved three factors, three levels, and 15 treatment combinations. Based on the fitting results, the quadratic model is significant and accurate in predicting the solid-liquid separation of Dypro 19 (p-value 0.0002, F-value 51.94, and R^2 0.9894). Numerical optimization based on the desirability function shows that using initial pH variables of 8, SEC dosage of 2.2 mL L^{-1}, and rapid stirring time of 3 min can produce a predicted removal of Dypro 19 of 97.01 %. Model validation through experiments on these variables shows that 95.71 % of Dypro 19 can be removed. These results indicate that the proposed model's validity, accuracy, and acceptability are good.

Keywords: Optimization, Flocculant performance, Flocculation, Starch-ethylene glycol dimethacrylate-chitosan, Response surface methodology, Box-Behnken design, Solid-liquid separation, Textile dye

1. Introduction

The availability of clean water is very important to support human life and socio-economic development [1]. As the home of humans and other living things, the earth provides clean water needed by living entities. However, with the progression of the era supported by population growth, and the intensity of industrialization that does not prioritize sustainability and climate change, the existence of clean water is increasingly threatened [2,3]. Currently, especially in cities in developing countries, the availability of clean water is increasingly vulnerable [1,4]; even more depressing, the existing of quality water sources are starting to be controlled by corporations [5]. As a result, the human right to water and sanitation in developing countries is difficult to realize because access to quality drinking water is limited [5,6]. Moreover, water pollution caused by industrial activities is often found in developing countries [7]. Pollutants in water are generally heavy metals and organic compounds [8].

Dyes used in industry, especially textile dyes, are one of the water pollutants that have received much

Received 4 September 2024; revised 23 November 2024; accepted 26 November 2024.
Available online 20 December 2024

* Corresponding author.
E-mail address: asepnurohmatmajalis@gmail.com (A.N. Majalis).

https://doi.org/10.33640/2405-609X.3388

attention because they are potentially toxic, carcinogenic, mutagenic, and generally not readily biodegradable [9–12]. In addition, dyes in water can limit sunlight's entry, reducing photosynthetic activity and thus affecting the entire aquatic biota [10–13], increasing chemical oxygen demand (COD), and changing the salinity and pH of water [9]. Therefore, dyes in water and wastewater must be removed before being discharged into streams.

Dypro Multi-Purpose Dye 19 Deep Blue or Dypro 19 is one dye used in the dyeing industry. This dye is suitable for dyeing natural fabrics such as cotton, linen, viscose, wool, silk, nylon, spandex, rayon, lycra, and 3D-printed items. It can also be used to dye buttons and feathers. The constituent ingredients of this dye and its hazard classification are presented in Table 1.

The removal of dyes from wastewater can be accomplished through physical, chemical, and biological processes or a combination of these processes [14]. Specifically, these processes are oxidation, ozonation, coagulation and flocculation, electrocoagulation, adsorption, photochemistry, membrane separation, and biological treatment [15]. Among these processes, coagulation-flocculation is the most widely applied due to its easy handling and high effectiveness, as well as low energy use and investment costs [16–18].

Recently, the development of biopolymer-based flocculants has become an attractive option to replace not only the Fe and Al-based coagulants but also the synthetic polymer-based flocculants [19–21]. As is well known, Fe and Al residues in water have negative impacts. Fe residues can reduce the service life of metal-based water treatment equipment, while Al residues can cause Alzheimer's disease [19,22]. Synthetic polymer residue from the flocculation process is also known to be toxic, potentially carcinogenic and not easily degraded in the environment [19]. Meanwhile, biopolymer-based flocculants have the advantage of being abundant in raw materials [23]. They are sustainable so that the cost can be cheaper [21,24], less hazardous [19,21], easily degraded naturally [24,25], and can act as coagulants and flocculants. For example, a ternary copolymer of starch-acrylic acid-chitosan copolymer (SAAC) has been able to reduce acid blue 113 dye by 99.7 % [25], and a ternary copolymer of starch-acrylic acid-itaconic acid (SAI) has been able to reduce crystal violet dye by 91.2 % [26].

Optimization of flocculation treatment parameters is necessary to improve the performance of biopolymer-based flocculants. Conventionally, the optimization process can be carried out using One Variable At a Time (OVAT) method [27,28]. However, the drawback of OVAT is that the correlation of various optimized parameters cannot be determined simultaneously, which results in a larger number of experiments and a longer time. Recently, the response surface methodology (RSM), as a more advanced experimental design, has been widely used to optimize coagulation-flocculation processes in wastewater treatment [18,27,29–32]. Optimization with RSM can simultaneously assess the relationship between the independent parameters and the expected measured response parameters to build a mathematical equation model so that the number of experiments is reduced and time can be shortened [27].

There are three types of response surface design, namely complete factorial design (FFD), central composite design (CCD), and box-Behnken design (BBD) [33–35]. Experiments using FFD must consider all possible combinations of all potential factor levels, so FFD requires many trials, which implies time and cost [33]. Therefore, CCD and BBD

Table 1. The ingredients content and its hazard classification in Dypro 19.

No	Ingredients	Hazard classification
1	Acid Blue 113 (disodium 8-anilino-5-[[4-[(3-sulfonatophenyl) diazenyl] naphthalen-1-yl] diazenyl] naphthalene-1-sulfonate) ($C_{32}H_{21}N_5Na_2O_6S_2$)	Eye Dam. 1:H318; Skin Sens. 1:H317
2	Direct Yellow 12 (disodium 4,4′-bis[(4-ethoxyphenyl) azo] stilbene-2,2′-disulphonate) ($C_{30}H_{28}N_4O_8S_2Na_2$)	Eye irrit. 2: H319
3	Disperse Yellow 42 (4-anilino-3-nitro-*N*-phenylbenzenesulfonamide) ($C_{18}H_{15}N_3O_4S$)	Skin Sens. 1:H137
4	Disperse Red 82 (2-[*N*-(2-acetyloxyethyl)-4-[(2-cyano-4-nitrophenyl) diazenyl] anilino] ethyl acetate) ($C_{21}H_{21}N_5O_6$)	Skin Sens. 1:H137

are often used in optimization [27]. The CCD method is usually used for two-level factor design, and each factor has five different levels. In CCD, axial points must be outside the 'cube' to test for possible extremes that are not in the desired region. BBD has only three different levels of factors. In BBD, there are no axial points outside the defined boundaries. Therefore, BBD is more practical because it has fewer design points and experimental tests than CCD [27].

In this study, the performance of the new biopolymer-based flocculant that can act as coagulant and flocculant, i.e. the starch chitosan cross-linked by ethylene glycol dimethacrylate or the starch-ethylene glycol dimetacrylate-chitosan, abbreviated as SEC, in removing Dypro 19 from wastewater was optimized using the response surface methodology box-Behnken design or RSM-BBD. The optimized treatment parameters were initial pH, SEC dosage, and rapid stirring time. The results showed that SEC could act as a coagulant and flocculant, removing Dypro 19 textile dye from wastewater up to 95.71 %.

2. Materials and methods

2.1. Materials

The materials used in this research included soluble starch (CAS No. 9905-84-9), acetic acid (CAS No. 64019-7), sodium hydroxide (CAS No. 1310-73-2), ethylene glycol dimethacrylate (EGDMA) (CAS No. 97-90-5), sulfuric acid (CAS No. 7664-93-9), and azobisisobutyronitrile (AIBN) (CAS No. 78-67-1), all in analytical grade, were obtained from Sigma–Aldrich. Low molecular weight chitosan (CAS No. 9012-76-4) with a degree of deacetylation of 75 % and a maximum limit of impurities of 10 % was obtained from Central Drug House (CDH). Ethanol (CAS No. 64-17-15) and acetonitrile (CAS No. 75-07-8), in analytical grade, were obtained from Merck. The textile dye, i.e., Dypro 19 deep blue multipurpose dye or Dypro 19 (Product code: 0101603119) was obtained from Professional Fabric Dyes Ltd.

2.2. Methods

2.2.1. Synthesis and characterization of SEC

2 g of starch was gradually dissolved in 60 mL of ultrapure water at 90 °C while stirring at 450 rpm. Then, the starch solution formed was cooled at room temperature and diluted in a 100 mL volumetric flask. Subsequently, the starch solution was mixed with EGDMA at a ratio of EGDMA: starch of 0.75 ml g^{-1}. The mixture was stirred at 850 rpm for 15 min at room temperature. Afterward, 50 mL of 2 % (w/v) chitosan solution in 1 % (v/v) acetic acid was added to the mixture and stirred at 850 rpm for 30 min at 60 °C. In the next step, AIBN, as the polymerization initiator, was added to the mixture (AIBN: starch mass ratio of 0.8 % g g^{-1}) and stirred at 850 rpm for 60 min at 60 °C. Finally, the mixture was poured into an autoclave and then polymerized at 90 °C for 5 h. The polymerized liquid was then named SEC and used for experiments in the optimization process.

For characterization, the polymer obtained (SEC) was precipitated by adding ethanol (ethanol: starch 2.5 mLg^{-1}) and left for 48 h. Furthermore, the precipitate and liquid were separated by centrifugation at 6500 rpm for 15 min. The precipitate obtained was dried at 50 °C for 24 h. Then, the dried precipitate was crushed and characterized by FTIR, XRD, and SEM.

FTIR (Brucker-Tensor II, US) was used to identify SEC functional groups and compare them with the functional groups of its constituent materials, i.e., starch, chitosan, and EGDMA. For FTIR analysis, each SEC powder, starch, chitosan, and the EGDMA liquid was mixed with KBr at room temperature and formed into pellets. FTIR analysis was performed in the wave number range of 4000–500 cm^{-1}, with a resolution of 2.0 cm^{-1} and a scan number of 45.

Furthermore, to identify the X-ray diffraction pattern and crystallinity of SEC and its constituent materials, an X-ray diffractometer (Malvern Panalytical AERIS, UK) with an X-ray source of copper, a scattering angle (2θ) of 5–85°, a scanning speed of 0.2°/second and a step size of 0.02°, was used, and the surface morphology of SEC and its constituent materials, i.e., starch and chitosan, was characterized using SEM (PhenomProx Desktop Scanning Electron Microscope, Thermo Fisher Scientific, US) by fixing a few drops of each powder on an iron stub of the SEM coated with gold. The zeta potential (ζ) of the dispersed material of SEC at pH 7 and Dypro 19 at pH 7 was measured by laser Doppler electrophoresis using a zeta potential analyzer (Horiba SZ 100, Javan) with a measurement range from −500 to +500 mV. Digital microscope VHX-5000 series (Keyence, Japan) is used for imaging the settled flocs from jar test experiment.

2.2.2. Experimental design and modelling

2.2.2.1. Single factor experiments. Single-factor experiments through jar tests were conducted to determine the range of the initial pH and SEC

dosage to be used for setting up the RSM-BBD experiment. The initial pH set in the single-factor experiment was 5, 6, 7, 8, and 9, and the fixed parameters were a flocculant dosage of 2 mL L^{-1}, wastewater volume of 500 mL, rapid stirring at 200 rpm for 2 min, slow stirring at 30 rpm for 15 min and sedimentation for 1 h. The SEC dosage set in the single-factor experiment was 1.4, 1.6, 1.8, 2.0, 2.2, 2.4, 2.6, 2.8, and 3.0 mL L^{-1}, and the fixed parameters used were an initial pH of 7, a wastewater volume of 500 mL, rapid stirring at 200 rpm for 2 min, slow stirring at 30 rpm for 15 min and sedimentation for 1 h.

2.2.2.2. The box-Behnken experimental design. RSM-BBD set-up and analysis were performed using Design Expert software 12 (State-Ease Inc., Minneapolis, US). The RSM-BBD experiment parameters are presented in Table 2. Three-factor levels of the BBD model were used to optimize Dypro 19 removal from wastewater. Three independent variables were selected: initial pH, SEC dosage, and rapid stirring time. Three levels (−1, 0, +1) of the independent variables were, respectively, A (initial pH of 7, 7.5, and 8), B (SEC dosage of 1.8, 2.4, and 2.6 mL L^{-1}), and C (rapid stirring time of 1, 3, and 5 min). Dypro 19 removal was the response of the optimization process. The total number of experiments performed is calculated using Equation (1) [27].

$$N = 2^{*}K(K-1) + C_0 \quad (1)$$

Where, K is the number of independent variables, and C_0 is the number of center points.

In this research, the number of center points is set at 3, so the number of experiments is 15. Each experiment was conducted three times, and the average of the responses obtained was used as the actual response value for each condition. The experimental data were then fitted using the second-order polynomial equation (Equation (2)) [27]. Furthermore, the effect of independent variables (linear, interaction, and quadratic) on the response was examined.

$$Y = \beta_0 + \sum_{i=1}^{k} \beta_i X_i + \sum_{i=1}^{k} \beta_{ii} X_i^2 + \sum_{i<j} \beta_{ij} X_i X_j + \varepsilon \quad (2)$$

Where Y is the response variable predicted by the model for the input of independent variables (X_i, X_j). $\beta_0, \beta_i, \beta_{ii}, \beta_{ij}$ are the regression coefficients for intercept, linear, quadratic, and interaction. And ε is the random error from different sources of variability.

Furthermore, the statistical significance of the equation model was tested by analysis of variance (ANOVA) through the F and p-value. The model fitting is expressed by R^2, adjusted R^2, and adequate precision value. The interaction of independent variables is shown by the 3D surface response plots and contours. Numerical optimization with desirability function is determined by setting input, i.e., initial pH "in range", SEC dosage "in range", rapid stirring time "in range", and the Dypro 19 removal as a response, "maximum". Finally, the numerical model was validated by conducting four experimental tests under optimum conditions.

2.2.3. The jar test procedure

In jar test experiments, wastewater was artificially made by dissolving 0.25 g Dypro 19 and then diluting it to 8 L. Each 500 mL of wastewater, conditioned for pH and SEC dosage, was poured into a beaker glass for the flocculation test. Next, the beaker glass was placed in a jar test apparatus (VELP Scientifica, Italy), which was run at a predetermined stirring speed and time.

2.2.4. Analytical techniques

The UV-visible spectrophotometer method (Agilent Cary 60 UV-visible, US) was used to evaluate the removal of Dypro 19 from wastewater. Wavelength scanning on a UV-visible spectrophotometer was carried out in the range of 400–800 nm to obtain the λ_{max} that resulted in the maximum absorbance of Dypro 19. Furthermore, the wastewater from each jar test result was determined for its absorbance at the maximum wavelength obtained. The standard reference used to determine the absorbance was

Table 2. The parameters set up and their respective levels of box-Behnken design for SEC optimization.

Independent variables (unit)	Symbol	Coded levels		
		Lower limit (−1)	Center (0)	Upper limit (+1)
Initial pH	A	7.0	7.5	8.0
SEC dosage (mL L^{-1})	B	1.8	2.2	2.6
Rapid stirring (minute)	C	1	3	5
Respond variable (unit)		Constrains		
Dye removal (%)	Y	Maximize		

ultrapure water. The removal of Dypro 19 from wastewater was calculated using Equation (3).

$$\text{Dypro 19 removal}\,(\%) = \frac{A_0 - A_t}{A_0} * 100 \qquad (3)$$

Where A_0 is the absorption of Dypro 19 before flocculation and A_t is the absorption of Dypro 19 after flocculation by SEC.

3. Results and discussion

3.1. The synthesis and characterization of SEC

SEC was synthesized by polymerizing starch and chitosan using EGDMA as a cross-linker and AIBN as an initiator. Polymerization was carried out under hydrothermal conditions without purging with N_2. The polymerization parameters used in the synthesis of SEC were the ratio of EGDMA: starch 0.75 mL g^{-1}, the ratio of starch: chitosan 2 g g^{-1}, and the ratio of AIBN: starch 0.8 % g g^{-1}.

The FTIR spectrum of SEC (Fig. 1) shows that it has functional groups derived from each of its constituents. SEC has functional groups that appear at specific wave numbers, namely: O–H (3292 cm^{-1}), C–H (2976 and 2944 cm^{-1}), C=O (1723 cm^{-1}), C=C (1636 cm^{-1}), N–H (1566 cm^{-1}), CH_3 and CH_2 (1451, 1382, 1321 and 1296 cm^{-1}), and C–O (1244 and 1015 cm^{-1}). Based on the FTIR spectrum of SEC, it is likely that the cross-linking between chitosan and EGDMA occurs in the NH_2 functional group, and the cross-linking between starch and EGDMA occurs in the CH_2–OH functional group. The NH_2 functional group does not appear in SEC, and the peak for the OH functional group in SEC has a lower intensity than that in starch. The similar result has also been reported by previous researchers, who explained that specific peaks of starch and chitosan appeared in the spectra of the prepared flocculant (starch–acrylic acid–chitosan (SAAC)) [25].

The X-ray diffraction patterns presented in Fig. 2 show that SEC appears more amorphous than starch and chitosan, and the crystallinity of chitosan is qualitatively higher than starch. The diffraction peak of starch at 16.89° indicates graminose type A starch. This type of starch has a semi-crystalline structure stabilized by intermolecular hydrogen bonds between starch macromolecules [36]. The diffraction peaks of chitosan appear at 19.98, 29.37, 31.65, and 45.39°. The diffraction peaks of starch and chitosan do not appear in SEC, and the tendency of the SEC diffraction pattern is amorphous. This indicates that cross-linking between starch, EGDMA, and chitosan produces a new amorphous compound, which strengthens the obtained FTIR characterization results.

SEM images of chitosan, starch, and SEC (Fig. 3), show that chitosan has a rougher surface than SEC, and the surface of SEC is rougher than starch. The

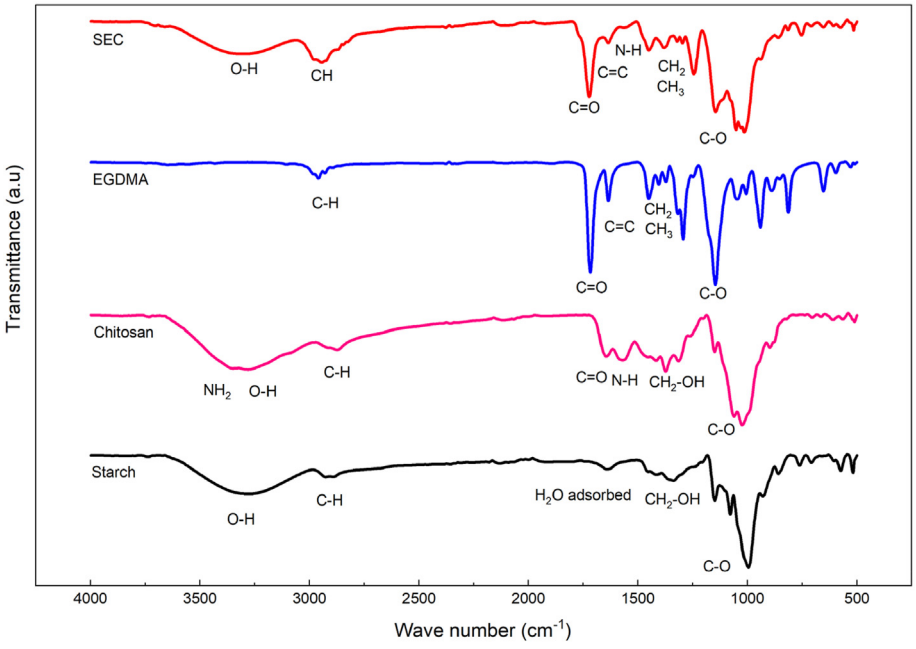

Fig. 1. The FTIR spectra of starch, chitosan, EGDMA and SEC.

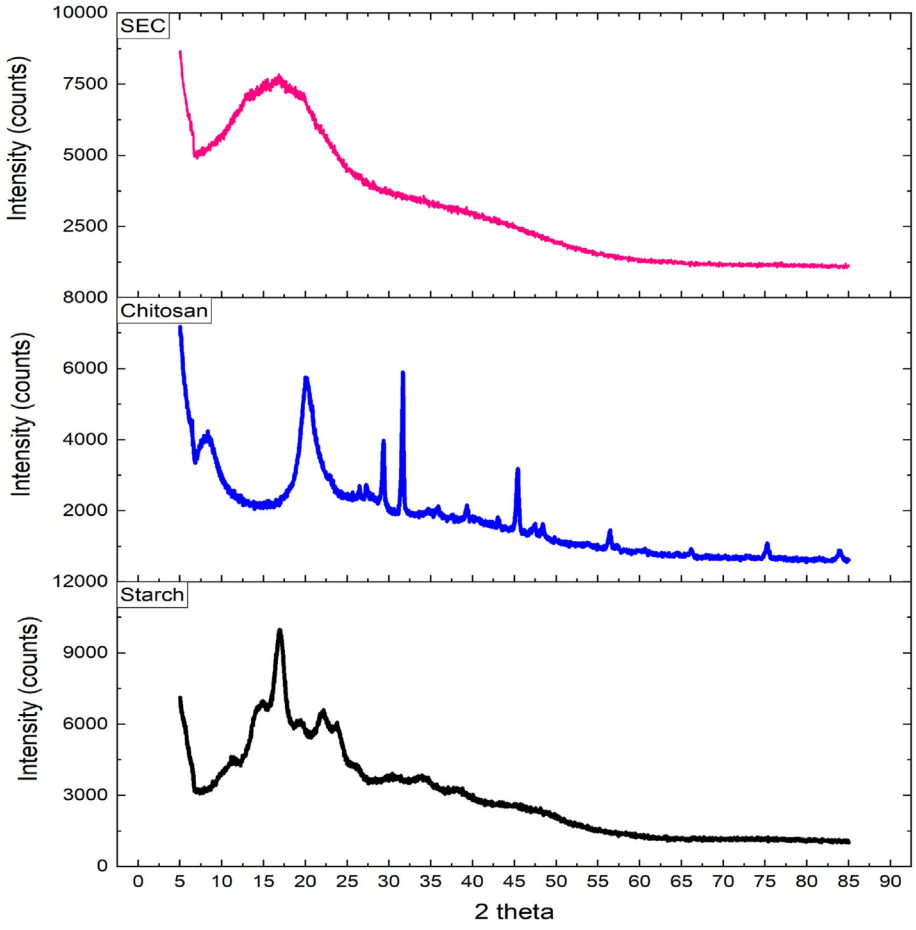

Fig. 2. The XRD spectra of starch, chitosan and SEC.

difference in surface roughness is obvious in SEM photos with a magnification of 10,000 times (Fig. 3a', Fig. 3b', and Fig. 3c'). Qualitatively, the shape of SEC looks like starch, which is spherical but large. SEM photos confirm the synthesis process using a starch: chitosan mass ratio of 2 g g^{-1}, which means the proportion of starch is twice that of chitosan; from SEM photos, it appears that the dominant structure of SEC is starch.

3.2. SEC performance test

The performance test of SEC flocculant in removing Dypro 19 from wastewater was evaluated by the UV-visible spectrophotometer method. The maximum absorbance of Dypro 19 was scanned from 400 to 800 nm. From the scanning results, the maximum absorbance of Dypro 19 was obtained at a wavelength of 588 nm, as presented in Fig. 4. Accordingly, a wavelength of 588 nm (λ_{max}) was set to determine the absorbance value during the experiment.

3.2.1. Single factor experiments

Generally, pH, temperature, coagulant dosage, and flocculant dosage significantly affect coagulation and flocculation performance. Then, the optimization process with RSM-BBD requires setting the lower and upper limits of independent parameters. Since SEC can act as both coagulant and flocculant, the single-factor experiment was only conducted on initial pH and SEC dosage.

Based on single factor experiments (Fig. 5a), Dypro 19 removal of 80.11 % was obtained at an initial pH of 7, and at the initial pH of 8, Dypro 19 removal changed to 77.61 %. In addition to the initial pH, the results according to Fig. 5a were obtained at fixed parameters, namely a SEC dosage of 2 mL L^{-1}, a rapid stirring of 200 rpm for 2 min, a slow stirring of 30 rpm for 15 min, and sedimentation for 1 h. The graph in Fig. 5a shows that with changes in initial pH, the Dypro 19 removal also changes significantly. These results indicate that changes in H^+ and OH^- derived from acids and bases will significantly determine the performance of SEC flocculants. This

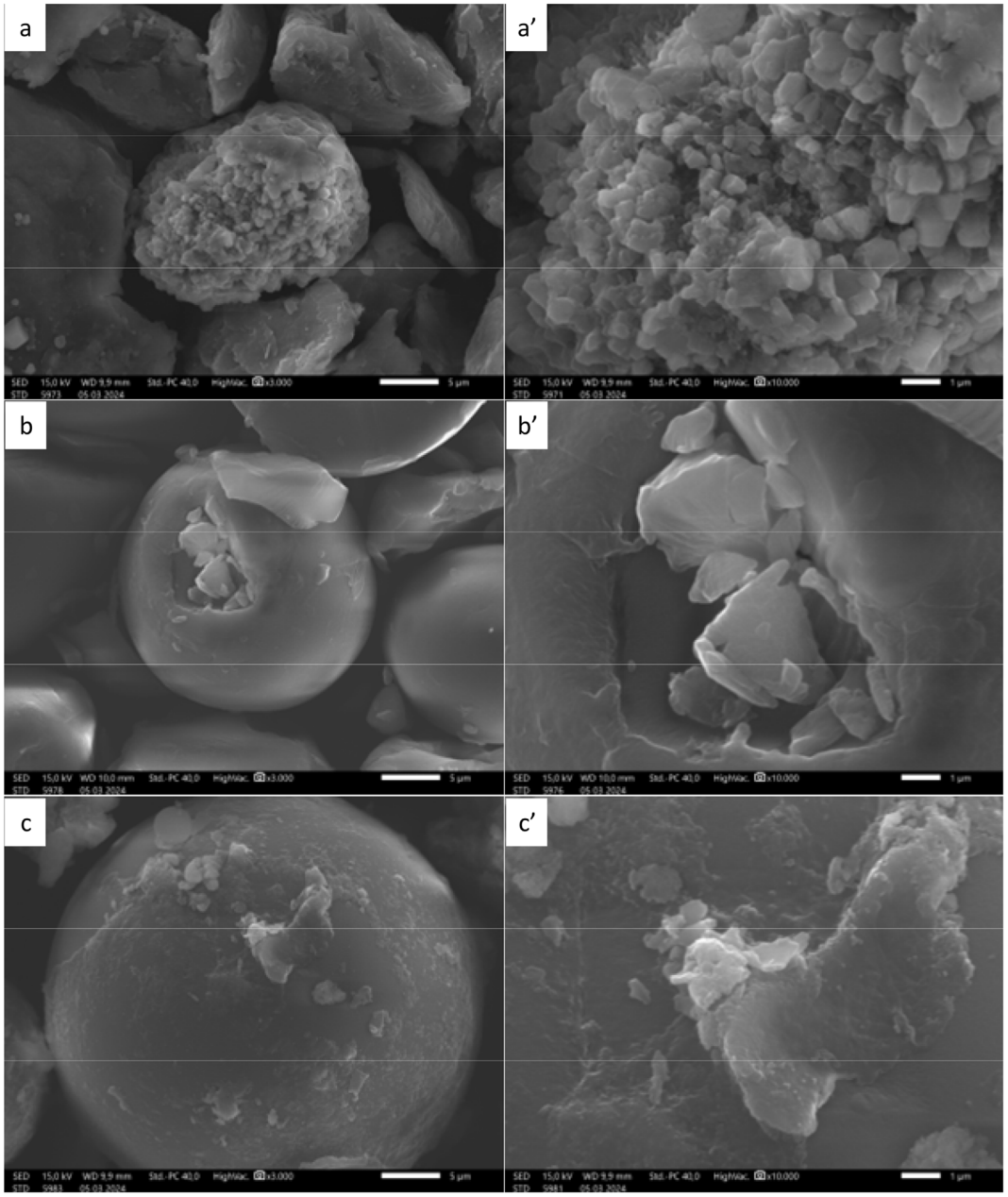

Fig. 3. SEM image of chitosan in magnification of 3000× (a) and 10,000× (a'), starch in magnification of 3000× (b) and 10,000× (b'), and SEC in magnification of 3000× (c) and 10,000× (c').

condition indicates that changes in pH will change the zeta potential value of the dye in wastewater so that it will change the optimum conditions of the dye removal process by SEC. This phenomenon indicates that one of the flocculation mechanisms by SEC is charge neutralization. To confirm the flocculation mechanism, the zeta potential values of SEC and Dypro 19 were measured at pH 7, and the results are shown in Fig. 6.

The flocculation performance of SEC is slightly different from that of previous reports that used SAI [26] and SAAC [25] biopolymer-based flocculants. The starch-acrylic acid-itaconic acid (SAI) based flocculant performs excellent flocculation in removing crystal violet dye under weakly acidic to neutral conditions. In contrast, the starch-acrylic acid-chitosan (SAAC) based flocculant has good flocculation performance in removing acid blue 113 dye in the pH range of 4–10. The differences in biopolymer-based flocculant performance highly depend on the degree of grafting and the type of monomers and crosslinkers. The degree of grafting

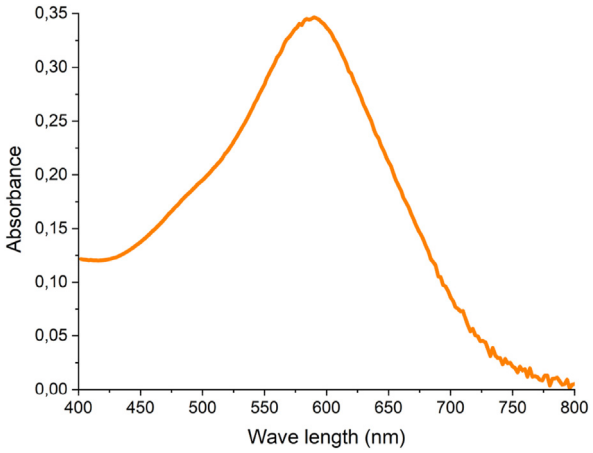

Fig. 4. The λ_{max} of Dypro 19.

indicates the composition of the monomers and crosslinkers. The type of monomers and crosslinkers will determine the particle charge of the biopolymer-based flocculant.

Dypro 19 removal by SEC as the effect of the dosage is presented in Fig. 5c. The dosage that produces the highest Dypro 19 removal is 2.4 mL L^{-1}. In the dosage from 2 to 2.4 mL L^{-1}, the change in Dypro 19 removal is not significant, respectively 92.18, 92.43 and 92.84 %. According to Fig. 5c the results were obtained at fixed parameters, i.e., initial pH 7, rapid stirring at 200 rpm for 2 min, slow stirring at 30 rpm for 15 min, and sedimentation for 1 h. The changes in the dosage that cause the changes in Dypro 19 removal can be understood from the flocculation mechanism, namely charge neutralization and adsorption. At low flocculant dosages, the adsorption and neutralization processes are not optimal, so the dye is still in the liquid phase. In optimum conditions, charge neutralization and adsorption occur, so the removal of the dye increases. In excessive dosages, which have implications for charge reversal, the dye that has been adsorbed and neutralized will stabilize again and come back to the liquid phase. In addition to charge neutralization and adsorption, a possible flocculation mechanism between SEC and Dypro 19 is interpolymer bridging [24], which is confirmed by the large size of the flocs, as presented in Fig. 7.

3.2.2. Optimization of the SEC performance

The jar test results from the single-factor experiment method were used as a base design in the experimental conditions for optimization with the RSM-BBD. The independent parameters chosen for variation in optimization with RSM-BBD were the initial pH, flocculant dosage, and rapid stirring time. At the same time, the response was the Dypro 19 removal, as presented in Table 2. The fixed parameters for the jar test process were as follows: 500 mL of wastewater, a dye concentration in the wastewater of approximately 31.25 mg L^{-1}, a rapid stirring at 200 rpm, a slow stirring at 30 rpm for 15 min, and sedimentation time for 1 h.

In this research, RSM-BBD was designed for three independent parameters, i.e., initial pH (7–8), SEC dose (1.8–2.6 mL L^{-1}), rapid stirring time (1–5 min), three center points, and 15 experiments. The effect of each independent parameter and its interaction on the response was investigated. Table 3 displays experimental conditions and the corresponding responses.

3.2.3. Model development

Three independent variables (A, B, and C) and a response variable (Y) are represented in a second-order polynomial-coded regression model, as shown in Equation (4) [28].

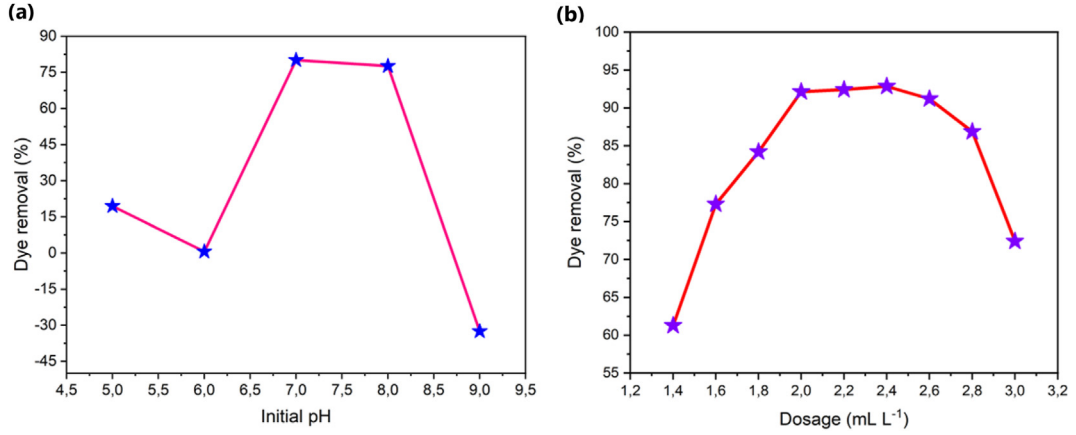

Fig. 5. The correlation of the initial pH (a) and SEC dosage (b) on the Dypro 19 removal obtained from single factor experiments.

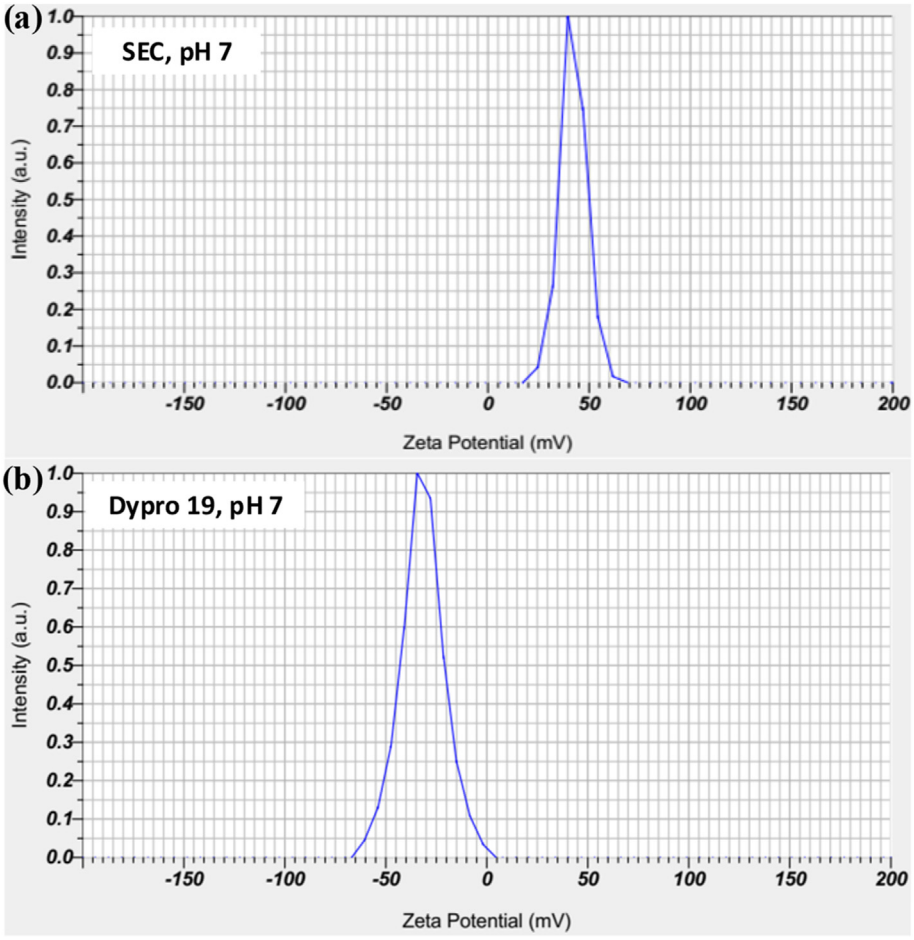

Fig. 6. The zeta potential of SEC (a) and Dypro 19 (b) at pH 7.

$$Y = \beta_0 + \beta_1 A + \beta_2 B + \beta_3 C + \beta_{12} AB + \beta_{13} AC + \beta_{23} BC + \beta_{11} A^2 + \beta_{22} B^2 + \beta_{33} C^2 \quad (4)$$

Where, β_0 is the regression coefficient, $\beta_{1,}\beta_{2,}\beta_3$ are linear coefficient, $\beta_{12,}\beta_{13,}\beta_{23}$ are interaction effect coefficient, $\beta_{11,}\beta_{22,}\beta_{33}$ are quadratic coefficient.

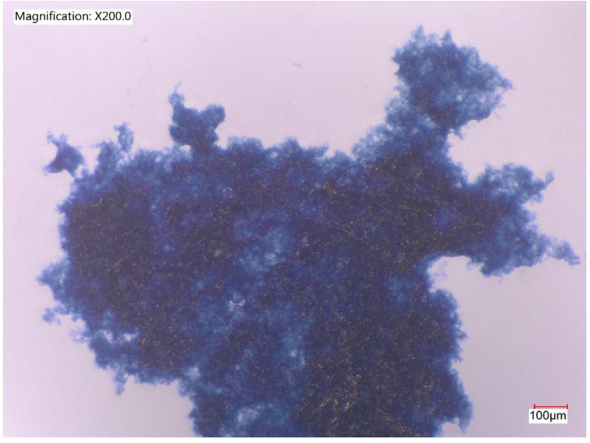

Fig. 7. The flocs formed from the destabilization of Dypro 19 by SEC.

The second-order response variable, representing Dypro 19 removal by SEC flocculant, can be expressed as an independent variable using the coded quadratic equation in Equation (5). This equation is obtained by performing a multi-regression analysis of the experimental data presented in Table 3.

$$Y = 87.28 + 12.75A - 16.78B + 2.9C + 20.01AB - 3.79AC + 1.92BC - 3.24A^2 - 14.35B^2 - 3.17C^2 \quad (5)$$

In this research, all coefficients in Equation (5) were used even though their influence on predicting the response variable was insignificant. Based on Equation (5), the value of Dypro 19 removal (Y) can be determined within the range of the BBD variable. According to the data in Table 3, the predicted value of Dypro removal obtained by the model is close to the experimental value. The diagnostic plot shows the relationship between the predicted data obtained from the model and the experimental data

Table 3. The box-Behnken design matrix with actual and predicted responses.

Run	Experimental conditions			Response (Y)	
	Initial pH (A)	SEC dosage (mL L^{-1}) (B)	Rapid stirring (minute) (C)	Dypro 19 removal (%)	
				Actual	Predicted
1	8 (+1)	2.2 (0)	1 (−1)	91.51	94.52
2	7 (−1)	2.6 (+1)	3 (0)	19.76	20.16
3	8 (+1)	2.6 (+1)	3 (0)	88.49	85.67
4	7 (−1)	2.2 (0)	1 (−1)	61.65	61.44
5	8 (+1)	2.2 (0)	5 (+1)	92.52	92.73
6	7 (−1)	1.8 (−1)	3 (0)	90.91	93.73
7	7.5 (0)	1.8 (−1)	1 (−1)	88.17	85.56
8	7.5 (0)	2.6 (+1)	5 (+1)	55.20	57.81
9	7.5 (0)	2.2 (0)	3 (0)	90.29	87.28
10	7.5 (0)	2.2 (0)	3 (0)	84.47	87.28
11	7.5 (0)	2.6 (0)	1 (−1)	48.36	48.17
12	7.5 (0)	1.8 (−1)	5 (+1)	87.34	87.53
13	7.5 (0)	2.2 (0)	3 (0)	87.09	87.28
14	7 (−1)	2.2 (0)	5 (+1)	77.83	74.82
15	8 (+1)	1.8 (−1)	3 (0)	79.62	79.22

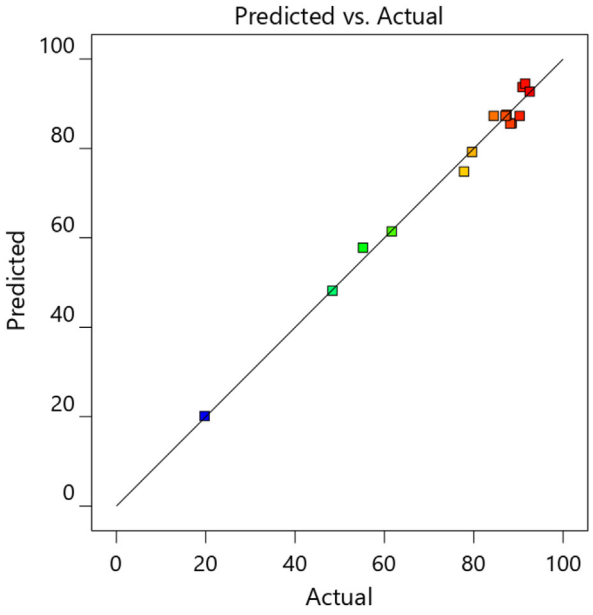

Fig. 8. The correlation between predicted and actual data of response (Dypro 19 removal).

(Fig. 8). The existing data points align closely with the diagonal line, indicating strong agreement between the experimental and predicted data [27,37].

3.2.4. Model verification through analysis of variance (ANOVA)

The statistical significance of the linear, interaction, and quadratic relationships between the independent and response variables is presented in Table 4. Based on the statistical model fitting results, the quadratic model with a sequential *p*-value of 0.0032 and an R^2 value of 0.9894 is more significant than the linear model (sequential *p*-value 0.0172), the 2-factor interaction model (2FI) (sequential *p*-value 0.0276), and the cubic model (sequential *p*-value 0.3649). The smaller the sequence *p*-value indicates, the more significant the model.

The R^2 value shows how much the dependent variable changes when the independent variable changes. It measures how accurately the model's predictions match the actual results. The R^2 value of 0.9894 indicates that more than 98 % of the variation in Dypro 19 removal is influenced by the independent variables (initial pH, SEC dosage, and rapid stirring time), and less than 2 % of the total variance cannot be explained by the model.

The response model for Dypro 19 removal (Y) exhibits a high F-value (51.94) with a relatively small *p*-value (0.0002), suggesting the model is suitable for analyzing and predicting results. A smaller *p*-value indicates that the related coefficient is significant in predicting results. Insignificant in the "Lack of Fit" of the model (*p*-value 0.3649) justifies the significance of the model. In Table 4, the F and *p*-values indicate the significance of the independent variables on Dypro 19 removal in the following sequence: SEC dosage (F-value 173.05 and *p*-value <0.0001), initial pH (F-value 99.91 and *p*-value 0.0002), and rapid stirring time (F-value 5.17 and *p*-value 0.0721).

The difference between the adjusted R^2 value and the predicted R^2 value is 0.102 (<0.2), indicating a reasonable agreement between the adjusted R^2 value and predicted values. Furthermore, the adequate precision value, indicating a strong signal and weak noise, is 25.2432. This value indicates that the model is acceptable because of >4. The adequate precision value in this research also indicates that

Table 4. ANOVA statistical results of the response surface quadratic model for Dypro 19 removal.

Source	Sum of Squares	df	Mean Square	F-value	p-value	
Model (Quadratic)	6083.58	9	675.95	51.94	0.0002	Significant
A = Initial pH	1300.25	1	1300.25	99.91	0.0002	
B = SEC dosage	2252.21	1	2252.21	173.05	<0.0001	
C= Rapid stirring	67.28	1	67.28	5.17	0.0721	
AB	1600.80	1	1600.80	123	0.0001	
AC	57.53	1	57.53	4.42	0.0895	
BC	14.71	1	14.71	1.13	0.3364	
A^2	38.74	1	38.74	2.98	0.1451	
B^2	760.24	1	760.24	58.41	0.0006	
C^2	37.03	1	37.03	2.84	0.1525	
Residual	65.07	5	13.01			
Lack of Fit	48.08	3	16.03	1.89	0.3649	Not significant
Pure error	16.99	2	8.50			
Corrected Total Sum of Square	6148.65	14				
Coefficient of variance (CV, %)	4.73					
R^2	0.9894					
Adjusted R^2	0.9704					
Predicted R^2	0.8687					
Adequate precision	25.2432					

the model's data prediction is reliable and can predict data within the design range. Additionally, the model's coefficient of variance (CV) value is 4.73 %, which indicates that the model is reproducible, accurate, and reliable. CV value is the ratio of the standard error to the mean value of the response.

3.2.5. The interactive effect of independent variables on Dypro 19 removal

The 3D surface and contour shown in Fig. 9 illustrate the interaction as a function of two independent variables in Dypro 19 removal, while the other at the center of the BBD is held constant. The 3D surface and contour's color variations indicate response values, with red representing the maximum response and blue representing the minimum response.

The interaction between the function of the initial pH and SEC dosage in the solid-liquid separation of Dypro 19 from wastewater at a fixed rapid stirring time variable of 3 min is shown in Fig. 9a. The interaction of the initial pH and SEC dosage effect is significant for Dypro 19 removal from wastewater. In the range of flocculant dosage parameters and an initial pH set, the higher the SEC dosage and the lower the initial pH of the treatment, Dypro 19 removal tended to decrease. An increase in SEC dosage accompanied by a decrease in pH implies an increase in the zeta potential value of the system so that the destabilization of Dypro 19 does not proceed appropriately. At pH 7, the potential zeta values of SEC and Dypro 19 were +42 mV and −37 mV, respectively (Fig. 6). With increasing SEC dose and decreasing pH, the zeta potential value of SEC became greater than +42 mV. The same thing happened to Dypro 19, with decreasing pH, the zeta potential value increased above −37 mV. So, the flocculation mechanism, namely charge neutralization, could not be achieved. The significance of the interaction between initial pH and SEC dosage (AB) on Dypro 19 removal was confirmed by the large F-value and the small *p*-value according to the results of the ANOVA analysis presented in Table 4.

Furthermore, Fig. 9b shows the interaction of initial pH and rapid stirring time in influencing Dypro 19 removal. The fixed variable in this condition is the SEC dosage of 2.2 mL L^{-1}. In the rapid stirring time range, the higher the initial pH, the higher the percentage of dye removal. Based on the F value of 4.42 and *p*-value of 0.0895, the interaction of initial pH and rapid stirring time (AC) in influencing Dypro 19 removal is quite significant.

Finally, the interaction of SEC dosage and rapid stirring time in removing the Dypro 19 at a fixed initial pH of 7.5 is shown in Fig. 9c. In the design rapid stirring time range, the higher the SEC dosage, the lower the percentage of Dypro 19 reduction. Likewise, the SEC dosage factor dominates the interaction of two factors. Based on the F value 1.13 and *p*-value 0.3364, the effect of the interaction of SEC dosage and rapid stirring time (BC) in removing Dypro 19 is lower than the effect of the interaction of initial pH with SEC dosage (AB) and the effect of the interaction of initial pH with rapid stirring time (AC).

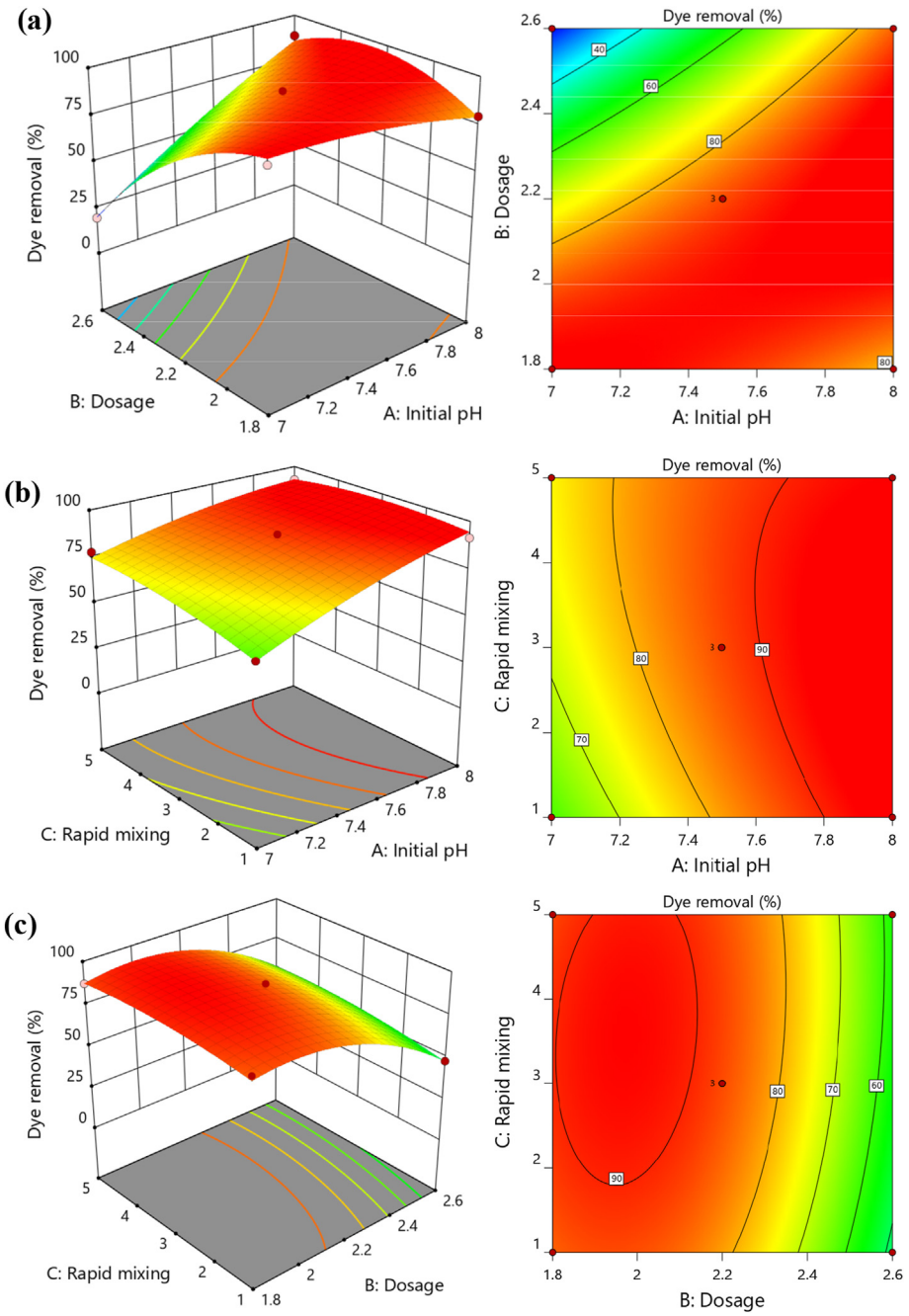

Fig. 9. 3D response surface plots and two-dimensional contour plots showing the effects of initial pH (A), SEC dosage (B), and rapid stirring time (C) on the Dypro 19 removal. (a) Response surface and contour plots of Dypro 19 removal as a function of A and B. (b) Response surface and contour plots of Dypro 19 removal as a function of A and C. (c) Response surface and contour plots of Dypro 19 removal as a function of B and C.

3.2.6. Numerical optimization using desirability function

This section uses numerical optimization using the desirability function to maximize Dypro 19 removal by simultaneously optimizing independent variables. *Desirability is* an objective function that has a value from 0 to 1. The closer to the value of '0', the further the response value is from the expected value, and the closer to the value of '1', the closer the response value is to the expected goal [27,38].

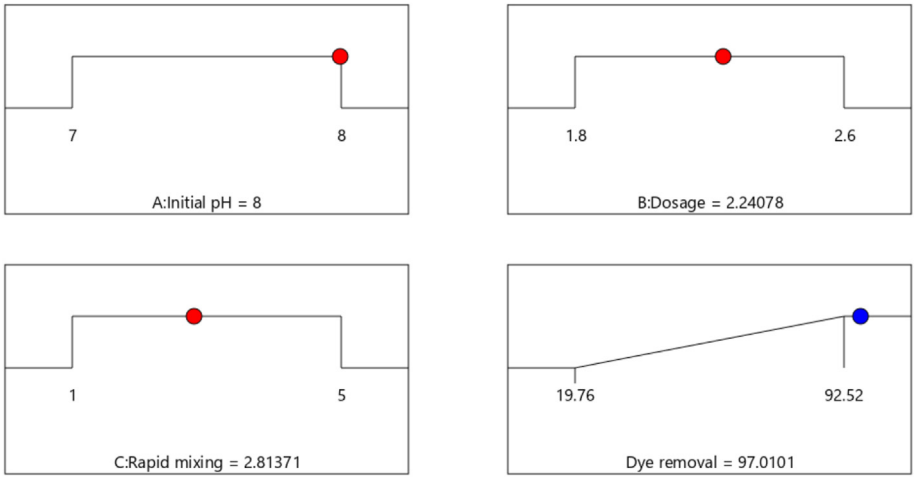

Fig. 10. The setting of independent parameters for numerical optimization using desirability function.

The numerical optimization is carried out by formulating independent variables "in range," while the response is set to "maximize".

According to the rump plots (Fig. 10), the optimized independent variables are the initial of 8, SEC dosage 2.24 mL L^{-1}–2.2 mL L^{-1}, and rapid stirring time 2.80754 min–3 min. The desirability of each optimized independent parameter is 1 (Fig. 11), indicating that all parameters are within the design range. The Dypro 19 removal as a response to the numerical optimization of independent parameters has a desirability value of 0.998796. If all independent parameters from the numerical optimization results are combined and used to produce a response, the target is the combined desirability value. Based on the numerical optimization of the independent parameters, a predicted response of 97.01 % was obtained. In addition, Fig. 12 shows two-dimensional contour plots and predicted responses under desirable conditions.

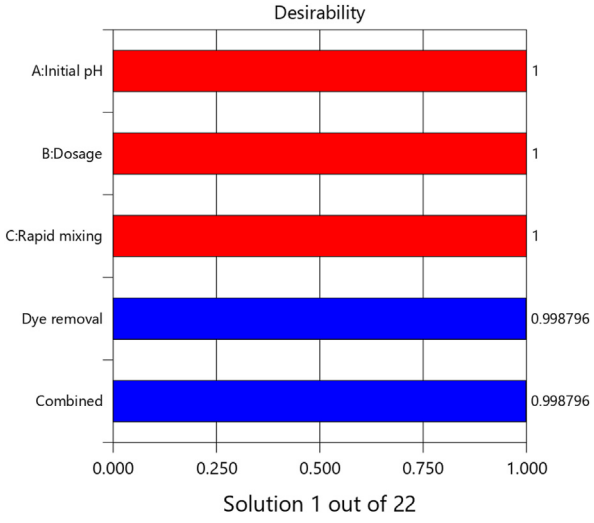

Fig. 11. The desirability of independent parameter and response based on numerical function from optimization.

3.2.7. Model validity by experiments

The four of experimental tests were conducted to verify the validity and predictability of the numerical optimization model. The difference between the predicted and actual responses was insignificant (Table 5). The Dypro 19 removal discrepancy between the actual and predicted data was 1.3 %. This result indicated that the quadratic model through RSM-BBD could predict results close to the actual values. A discrepancy below 10 % is acceptable in experiments related to flocculation parameters [18,39]. Therefore, the model proposed in this study is reliable and applicable within the specified design range.

3.2.8. Comparison with relevant flocculant

The comparison of the SEC synthesis method and its flocculation performance with other biopolymer-based flocculants and conventional coagulants is presented in Table 6. SEC has the advantage of being a simple synthesis process and environmentally friendly material, but it can also remove composite dyes from wastewater. Generally, the dyes used in the textile industry are combined or composite dyes. Dypro 19 used in this study is a composite dye, as presented previously in Table 1.

In terms of its constituent materials, SEC is composed of more environmentally friendly

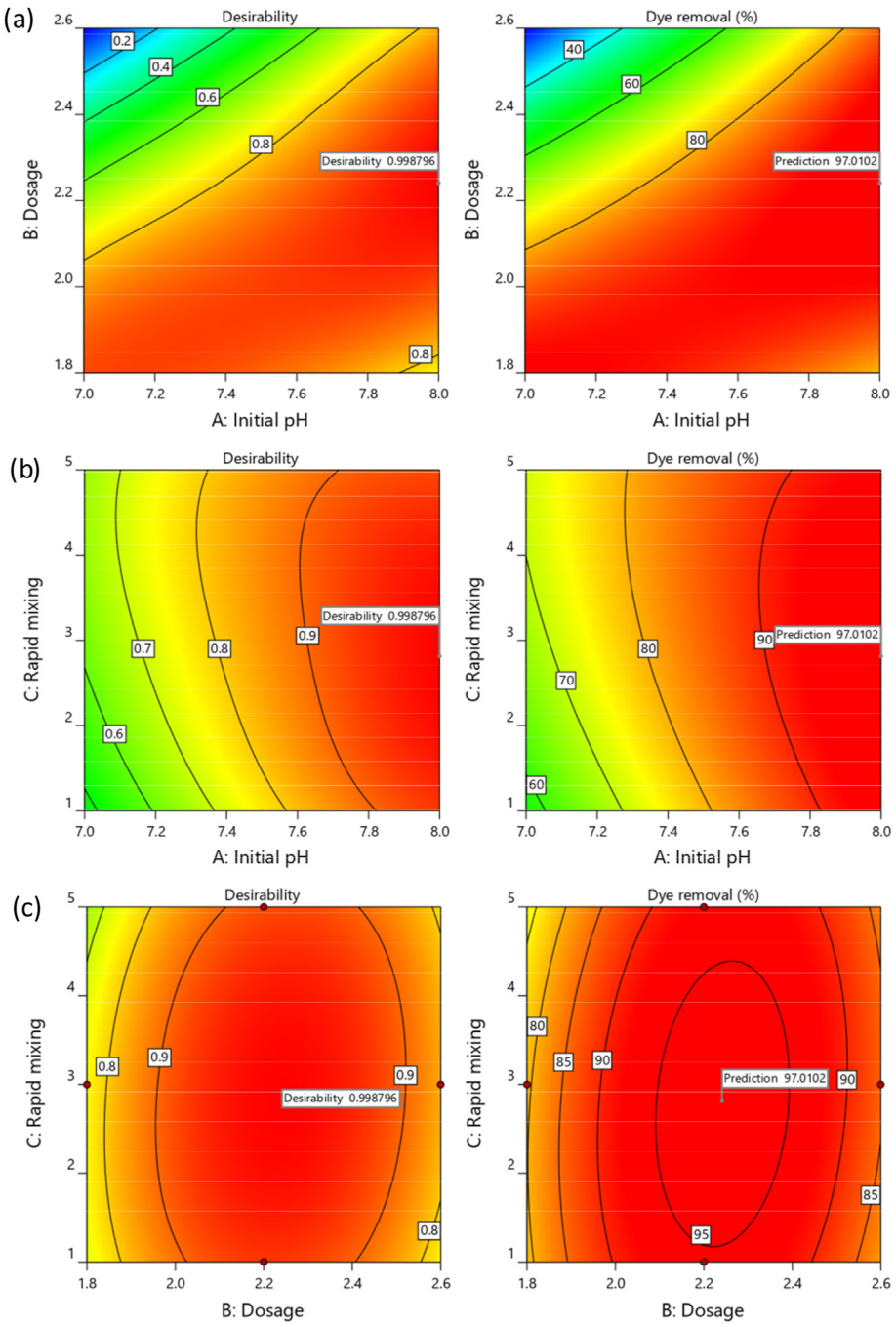

Fig. 12. 2D contour plots of desirability and the prediction of Dypro 19 removal.

Table 5. Validation of predicted results by experiments under optimum conditions.

Response	Mean ± SD	
	Actual	Predicted
Dye removal (%)	95.71 ± 1,08	97.01

SD = standard deviation (n = 4).

materials. Starch and chitosan, as monomers of SEC, are natural materials. EGDMA is used as a crosslinker and has lower toxicity to aquatic organisms than acrylic acid or acrylamide. AIBN, as the initiator in the synthesis of SEC, is also less harmful than cerium ammonium nitrate.

Table 6. The comparison of SEC with relevant flocculant.

Flocculant[a]	Synthesis and preparation process	Performance	Ref
SEC	Initiator AIBN, 90 °C, 5 h, without N_2 atmosphere.	SEC has high-performance flocculation for removing Dypro 19 (the composite dye from Acid Blue 113, Direct Yellow 12, Disperse Yellow 42, and Disperse Red 82). Optimum variables: dosage 2.2 mL L^{-1}, pH 8 and rapid stirring time 3 min. Dye removal achieved 95.71 %.	This work
SAI	Neutralization degree of acrylic acid 70 % by sodium hydroxide, composite initiator of $NaHSO_3$ dan $(NH_4)_2S_2O_8$. N_2 atmosphere, room temperature, 5 h	SAI showed high crystal violet color removal efficiency at wide pH, temperature, and ionic strength scopes. The SAI dose of 25 mg/L reduced 100 mg/L CV by 91.2 %.	[26]
SAAC	Neutralization degree of acrylic acid 70 % by sodium hydroxide, initiator cerium ammonium nitrate, 50 °C, N_2 atmosphere, 5 h	SAAC has High-performance flocculation for removing acid blue 113 (up to 99.7 %) at a wide range of pH and flocculant dosage. The ratio of optimal flocculant dosage to the initial dye concentration was 2.0, 2.0, 1.5, and 1.67 for the initial dye concentrations of 25, 50, 100, and 150 mg/L.	[25]
CAMFA	Dual initiator (K_2S2O8 and Na2S2O3), 60 °C, 5 h	The flocculation performance of CAMFA in reducing Acid blue 113, reactive black, and methyl orange was 97.0 %, 91.6 %, and 38.2 %, respectively, at a dose of 283 mg/L CAMFA for 100 mg/L dye.	[40]
CGSt	Corn starch as raw material, methacryloyloxyethyl trimethyl ammonium chloride (DMC) as cationization agent grafting monomer, N.N′-methylenebisacrylamide (MBA) as crosslinking monomer. Initiator Fenton (containing H_2O_2 and $FeCl_2$.Fe_2O). Crosslinking-grafting copolymerization at 35 °C, 1.5 h	CGSt has high-performance flocculation for removing Acid Light Yellow G, Direct Lake Blue 5B, and Reactive Brilliant Blue KE-GN. The dye removal achieved is 97.2 % (Acid Light Yellow G), 96.3 % (Direct Lake Blue 5B), and 97.2 % (Reactive Brilliant Blue KE-GN). The optimum pH is 9, and the optimum dosage ranges from 5 to 12 g/L. The dye concentration is 300 mg/L.	[36]
g-AP	Free radical polymerization, initiator potassium persulphate (KPS), 65 °C, N_2 atmosphere, 1 h.	g-AP has high-performance flocculation for methylene blue and reactive blue. The optimum variables for removing methylene blue are pH 9, dosage 9 ppm, and dye concentration 30 mg/L. The optimum variables for reactive blue removal are pH 4, dosage 9 ppm, and dye concentration 30 mg/L.	[41]
$FeCl_3$, $AlCl_3$, dan natural coagulant Okra pods	$FeCl_3$ and $AlCl_3$ prepared by diluting 1 g of these salts in 1 L of deionized water. Washed Okra pods dried in oven at 45 °C, 24 h. Grinding until 150 μm. Furthermore, 1 g Okra pods powder is diluted in 1 L distilled water	$FeCl_3$, $AlCl_3$, and Okra pods can remove Vat Green 3 dye by 97.3, 94.5, and 92.5 %, respectively. At an 80 mg/L dye concentration, the optimum pH and dosage are $FeCl_3$ (pH 6, dosage 400 mg/L), $AlCl_3$ (pH 7, dosage 400 mg/L), and Okra pods (pH 6, dosage 200 mg/L).	[42]

[a] SAAC (starch-acrylic acid-chitosan), CAMFA (chitosan-acrylamide-fulvic acid), CGSt (cross-linked grafted cationic starch flocculant), g-AP (amylopectin grafted with poly acrylic acid), SAI (starch-acrylic acid-itaconic acid).

4. Conclusion

Optimization of SEC flocculant performance in solid-liquid separation of Dypro 19 by RSM-BBD was carried out on the independent variables of initial pH (A), SEC dosage (B), and rapid stirring time (C). SEC can effectively remove Dypro 19 because it has a positive particle charge, its surface is quite rough, and it has functional groups such as O–H, C=O, C=C, N–H, and C–O, which can facilitate destabilization, polymer bridging, and adsorption of Dypro 19. Based on the fitting results, the quadratic model has a good significance and degree of accuracy in predicting the solid-liquid separation of Dypro 19 from wastewater (p-value 0.0002, F value 51.94, and R^2 0.9894). The interaction between initial pH and SEC dosage (AB) had a more significant effect on solid-liquid separation of Dypro 19 than the interaction between SEC dosage and rapid stirring time (BC) and the interaction between initial pH and rapid stirring time (AC). Numerical optimization based on the desirability function showed that the use of

variable initial pH 8, SEC dosage 2.2 mL L^{-1}, and rapid stirring time of 3 min can produce a predicted Dypro 19 removal of 97.01 %. Validation of the model through experiments on these variables shows that the actual Dypro 19 removal that can be obtained is 95.71 %. These results indicate that the validity, accuracy, and acceptability of the proposed model are good.

Ethics information

None.

Funding

This research was funded by the Research Organization for Life Sciences and Environment, National Research and Innovation Agency, Indonesia, through the scheme of the 2023 Home Program for the Disclosure and Utilization of the Archipelago's Biodiversity (FUND ID. RP1TP3SubTheme1).

Acknowledgements

The authors acknowledge the facilities, scientific and technical support from Advanced Characterization Laboratories of National Research and Innovation Agency, Indonesia.

References

[1] S.M. Praveena, A.Z. Aris, Z. Hashim, J.H. Hashim, Drinking water quality status in Malaysia: a scoping review of occurrence, human health exposure, and potential needs, J. Expo. Sci. Environ. Epidemiol. 34 (2024) 161–174, https://doi.org/10.1038/s41370-023-00585-3.

[2] S. Lebu, A. Lee, A. Salzberg, V. Bauza, Adaptive strategies to enhance water security and resilience in low- and middle-income countries: a critical review, Sci. Total Environ. 925 (2024) 1–21, https://doi.org/10.1016/j.scitotenv.2024.171520.

[3] D. Naderian, R. Noori, E. Heggy, S.M. Bateni, R. Bhattarai, A. Nohegar, S. Sharma, A water quality database for global lakes, Resour. Conserv. Recycl. 202 (2024) 1–8, https://doi.org/10.1016/j.resconrec.2023.107401.

[4] S. Olmstead, J. Zheng, Water pollution control in developing countries: policy instruments and empirical evidence, Rev. Environ. Econ. Policy 15 (2021) 261–280, https://doi.org/10.1086/715645.

[5] H. Johnson, N. South, R. Walters, The commodification and exploitation of fresh water: property, human rights and green criminology, Int. J. Law Crime Justice 44 (2016) 146–162, https://doi.org/10.1016/j.ijlcj.2015.07.003.

[6] D.A. Senna, V.R. Moreira, M.C.S. Amaral, E.C. de Paula, L.P. Pereira, R.M.G. Batista, L.A.F. Ferreira, S. Rezende, Industry 4.0 as a strategy to contribute to the water supply universalization in developing countries, J. Environ. Chem. Eng. 11 (2023) 1–13, https://doi.org/10.1016/j.jece.2023.111198.

[7] Z. Yang, B. Li, R. Xia, S. Ma, R. Jia, C. Ma, L. Wang, Y. Chen, L. Bin, Understanding China's industrialization driven water pollution stress in 2002–2015—a multi-pollutant based net gray water footprint analysis, J. Environ. Manag. 310 (2022) 1–13, https://doi.org/10.1016/j.jenvman.2022.114735.

[8] H. de A.G. dos Santos, R.S.A. Kitamura, G. da C.B. Soares, M.P. dos Santos, L.P. de S. Miranda, M. Mela, J.R.S. Vitule, M.T. Grassi, M.M. Cestari, A.A. Padial, H.C. Silva de Assis, Assessing the water quality in a World Heritage Site using biomarkers in top fish predators, Sci. Total Environ. 927 (2024) 1–16, https://doi.org/10.1016/j.scitotenv.2024.172072.

[9] T. Tomar, N. Kahandawala, J. Kaur, L. Thounaojam, I. Choudhary, S. Bera, Bioremediation of synthetic dyes from wastewater by using microbial nanocomposites: an emerging field for water pollution management, Biocatal. Agric. Biotechnol. 51 (2023) 1–12, https://doi.org/10.1016/j.bcab.2023.102767.

[10] S. Dutta, S. Adhikary, S. Bhattacharya, D. Roy, S. Chatterjee, A. Chakraborty, D. Banerjee, A. Ganguly, S. Nanda, P. Rajak, Contamination of textile dyes in aquatic environment: adverse impacts on aquatic ecosystem and human health, and its management using bioremediation, J. Environ. Manag. 353 (2024) 1–22, https://doi.org/10.1016/j.jenvman.2024.120103.

[11] S. Deniz, Efficient and environmentally friendly removal of azo textile dye using a low-cost adsorbent: kinetic and reuse studies with application to textile effluent, Mater. Today Commun. 35 (2023) 1–10, https://doi.org/10.1016/j.mtcomm.2023.106433.

[12] B. Lellis, C.Z. Fávaro-Polonio, J.A. Pamphile, J.C. Polonio, Effects of textile dyes on health and the environment and bioremediation potential of living organisms, Biotechnol. Res. Innov. 3 (2019) 275–290, https://doi.org/10.1016/j.biori.2019.09.001.

[13] J. Lin, W. Ye, M. Xie, D.H. Seo, J. Luo, Y. Wan, B. Van der Bruggen, Environmental impacts and remediation of dye-containing wastewater, Nat. Rev. Earth Environ. 4 (2023) 785–803, https://doi.org/10.1038/s43017-023-00489-8.

[14] B.Y. Patel, H.K. Patel, Current approaches toward the removal of methylene blue dye from synthetic textile effluent using bacterial treated agricultural waste absorbent through statistical design, Heliyon 9 (2023) e19857, https://doi.org/10.1016/j.heliyon.2023.e19857, 1–14.

[15] F.H.A. Mustafa, E.K.M. Gad ElRab, R.M. Kamel, R.F.M. Elshaarawy, Cost-effective removal of toxic methylene blue dye from textile effluents by new integrated crosslinked chitosan/aspartic acid hydrogels, Int. J. Biol. Macromol. 248 (2023) 1–14, https://doi.org/10.1016/j.ijbiomac.2023.125986.

[16] X. Jiang, Y. Li, X. Tang, J. Jiang, Q. He, Z. Xiong, H. Zheng, Biopolymer-based flocculants: a review of recent technologies, Environ. Sci. Pollut. Res. 28 (2021) 46934–46963, https://doi.org/10.1007/s11356-021-15299-y.

[17] Y. Sun, D. Li, X. Lu, J. Sheng, X. Zheng, X. Xiao, Flocculation of combined contaminants of dye and heavy metal by nano-chitosan flocculants, J. Environ. Manag. 299 (2021) 1–9, https://doi.org/10.1016/j.jenvman.2021.113589.

[18] H. Shabanizadeh, M. Taghavijeloudar, A sustainable approach for industrial wastewater treatment using pomegranate seeds in flocculation-coagulation process: optimization of COD and turbidity removal by response surface methodology (RSM), J. Water Process Eng. 53 (2023) 1–13, https://doi.org/10.1016/j.jwpe.2023.103651.

[19] N. Das, N. Ojha, S.K. Mandal, Wastewater treatment using plant-derived bioflocculants: green chemistry approach for safe environment, Water Sci. Technol. 83 (2021) 1797–1812, https://doi.org/10.2166/wst.2021.100.

[20] S.Y. Choy, K.M.N. Prasad, T.Y. Wu, M.E. Raghunandan, R. N. Ramanan, Utilization of plant-based natural coagulants as future alternatives towards sustainable water clarification, J. Environ. Sci. (China) 26 (2014) 2178–2189, https://doi.org/10.1016/j.jes.2014.09.024.

[21] B. Zaman, N. Hardyanti, M. Arief Budiharjo, S. Budi Prasetyo, A. Ramadhandi, A.T. Listiyawati, Natural flocculant vs chemical flocculant where is better to used in wastewater treatment, in: IOP Conf Ser Mater Sci Eng, Institute of Physics Publishing. 2020, pp. 1–5, https://doi.org/10.1088/1757-899X/852/1/012014.

[22] S. Mohd Asharuddin, N. Othman, W.A.H. Altowayti, N. Abu Bakar, A. Hassan, Recent advancement in starch modification and its application as water treatment agent, Environ. Technol. Innov. 23 (2021) 1–23, https://doi.org/10.1016/j.eti.2021.101637.

[23] H. Zhang, G. Guan, T. Lou, X. Wang, High performance, cost-effective and ecofriendly flocculant synthesized by grafting carboxymethyl cellulose and alginate with itaconic acid, Int. J. Biol. Macromol. 231 (2023) 1–8, https://doi.org/10.1016/j.ijbiomac.2023.123305.
[24] M.A.A. Razali, A. Ariffin, Polymeric flocculant based on cassava starch grafted polydiallyldimethylammonium chloride: flocculation behavior and mechanism, Appl. Surf. Sci. 351 (2015) 89–94, https://doi.org/10.1016/j.apsusc.2015.05.080.
[25] J. Xun, T. Lou, J. Xing, W. Zhang, Q. Xu, J. Peng, X. Wang, Synthesis of a starch–acrylic acid–chitosan copolymer as flocculant for dye removal, J. Appl. Polym. Sci. 136 (2019) 1–7, https://doi.org/10.1002/app.47437.
[26] J. Qin, X. Wang, T. Lou, Economic and environmentally friendly anionic flocculant synthesized by starch-acrylic acid-itaconic acid grafting and efficient treatment of cationic dye wastewater, Colloids. Surf. A Physicochem. Eng. Asp. 699 (2024) 1–10, https://doi.org/10.1016/j.colsurfa.2024.134708.
[27] T.A.O.K. Meetiyagoda, T. Takahashi, T. Fujino, Response surface optimization of chemical coagulation for solid-liquid separation of dairy manure slurry through Box–Behnken design with desirability function, Heliyon 9 (2023) e17632, https://doi.org/10.1016/j.heliyon.2023.e17632, 1–16.
[28] M. Yan, D. Wang, J. Yu, J. Ni, M. Edwards, J. Qu, Enhanced coagulation with polyaluminum chlorides: role of pH/Alkalinity and speciation, Chemosphere 71 (2008) 1665–1673, https://doi.org/10.1016/j.chemosphere.2008.01.019.
[29] A. Benalia, O. Baatache, K. Derbal, A. Khalfaoui, Z. Amrouci, A. Pizzi, A. Panico, The use of central composite design (CCD) to optimize and model the coagulation-flocculation process using a natural coagulant: application in jar test and semi-industrial scale, J. Water Process. Eng. 57 (2024) 1–17, https://doi.org/10.1016/j.jwpe.2023.104704.
[30] C. Kang, Y. Zhao, C. Tang, O. Addo-Bankas, Use of aluminum-based water treatment sludge as coagulant for animal farm wastewater treatment, J. Water Process. Eng. 46 (2022) 1–9, https://doi.org/10.1016/j.jwpe.2022.102645.
[31] N.M. Huzir, M.M.A. Aziz, S.B. Ismail, N.A.N. Mahmood, N. A. Umor, S.A. Faua'ad Syed Muhammad, Optimization of coagulation-flocculation process for the palm oil mill effluent treatment by using rice husk ash, Ind. Crops. Prod. 139 (2019) 1–9, https://doi.org/10.1016/j.indcrop.2019.111482.
[32] A.A.K. Dhrubo, M. Jannat, M.S. Hossain, Enhancing the performance of coagulants for wastewater treatment by varying and optimizing the experimental parameters, J. Water Process. Eng. 55 (2023) 1–12, https://doi.org/10.1016/j.jwpe.2023.104144.
[33] I. Veza, M. Spraggon, I.M.R. Fattah, M. Idris, Response surface methodology (RSM) for optimizing engine performance and emissions fueled with biofuel: review of RSM for sustainability energy transition, Results Eng. 18 (2023) 1–14, https://doi.org/10.1016/j.rineng.2023.101213.
[34] R.K. Ahmed, E.M. Saad, H.M. Fahmy, R.M. El Nashar, Multivariate experimental design: towards more reliable electrochemical detection, Curr. Opin. Electrochem. 31 (2022) 1–12, https://doi.org/10.1016/j.coelec.2021.100880.
[35] L.M.S. Pereira, T.M. Milan, D.R. Tapia-Blácido, Using Response Surface Methodology (RSM) to optimize 2G bioethanol production: a review, Biomass Bioenergy 151 (2021) 1–14, https://doi.org/10.1016/j.biombioe.2021.106166.
[36] H. Zhang, J. Li, S. Cao, Y. Ding, H. Wang, N. Chang, Preparation of crosslinking - grafting cationic starch flocculant and its study on textile dyes removal, J. Polym. Environ. 32 (2024) 3407–3421, https://doi.org/10.1007/s10924-023-03133-0.
[37] K. Thirugnanasambandham, R.R. Karri, Preparation and characterization of Azadirachta indica A. Juss. plant based natural coagulant for the application of urban sewage treatment: modelling and cost assessment, Environ. Technol. Innov. 23 (2021) 1–12, https://doi.org/10.1016/j.eti.2021.101733.
[38] D.E.G. Trigueros, L. Braun, C.L. Hinterholz, Environmental and economic feasibility of the treatment of dairy industry wastewater by photo-Fenton and electrocoagulation process: multicriteria optimization by desirability function, J. Photochem. Photobiol. Chem. 427 (2022) 1–14, https://doi.org/10.1016/j.jphotochem.2022.113820.
[39] B.L. Choong Lek, A.P. Peter, K.H. Qi Chong, P. Ragu, V. Sethu, A. Selvarajoo, S.K. Arumugasamy, Treatment of palm oil mill effluent (POME) using chickpea (Cicer arietinum) as a natural coagulant and flocculant: evaluation, process optimization and characterization of chickpea powder, J. Environ. Chem. Eng. 6 (2018) 6243–6255, https://doi.org/10.1016/j.jece.2018.09.038.
[40] T. Lou, X. Wang, G. Song, G. Cui, Synthesis and flocculation performance of a chitosan-acrylamide-fulvic acid ternary copolymer, Carbohydr. Polym. 170 (2017) 182–189, https://doi.org/10.1016/j.carbpol.2017.04.069.
[41] A.K. Sarkar, S. Ghorai, A.S. Patra, B.K. Mishra, N.R. Mandre, S. Pal, Modified amylopectin based flocculant for the treatment of synthetic effluent and industrial wastewaters, Int. J. Biol. Macromol. 72 (2014) 356–363, https://doi.org/10.1016/j.ijbiomac.2014.08.019.
[42] T.K. Hussein, Removal of vat green 3 dye from aqua solution using chemical coagulants and okra pods as natural coagulant by coagulation-flocculation process, Pollution 9 (2023) 1638–1652, https://doi.org/10.22059/POLL.2023.358029.1875.